

Separating poroviscoelastic deformation mechanisms in hydrogels

Daniel G. T. Strange, Timothy L. Fletcher, Khaow Tonsomboon, Helen Brawn, Xuanhe Zhao et al.

Citation: *Appl. Phys. Lett.* **102**, 031913 (2013); doi: 10.1063/1.4789368

View online: <http://dx.doi.org/10.1063/1.4789368>

View Table of Contents: <http://apl.aip.org/resource/1/APPLAB/v102/i3>

Published by the [American Institute of Physics](#).

Related Articles

Shear behavior of a confined thin film: Influence of the molecular dynamics scheme employed
J. Chem. Phys. **138**, 054707 (2013)

Thermodynamic properties of liquid water from a polarizable intermolecular potential
J. Chem. Phys. **138**, 044503 (2013)

Probing viscosity of nanoliter droplets of butterfly saliva by magnetic rotational spectroscopy
Appl. Phys. Lett. **102**, 033701 (2013)

Relaxation processes in liquids: Variations on a theme by Stokes and Einstein
J. Chem. Phys. **138**, 12A526 (2013)

Entangled triblock copolymer gel: Morphological and mechanical properties
J. Chem. Phys. **138**, 024908 (2013)

Additional information on *Appl. Phys. Lett.*

Journal Homepage: <http://apl.aip.org/>

Journal Information: http://apl.aip.org/about/about_the_journal

Top downloads: http://apl.aip.org/features/most_downloaded

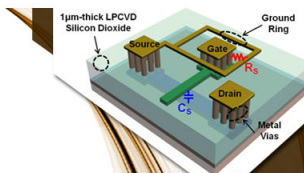
Information for Authors: <http://apl.aip.org/authors>

ADVERTISEMENT



**EXPLORE WHAT'S
NEW IN APL**

SUBMIT YOUR PAPER NOW!



SURFACES AND INTERFACES

Focusing on physical, chemical, biological, structural, optical, magnetic and electrical properties of surfaces and interfaces, and more...



ENERGY CONVERSION AND STORAGE

Focusing on all aspects of static and dynamic energy conversion, energy storage, photovoltaics, solar fuels, batteries, capacitors, thermoelectrics, and more...

Separating poroviscoelastic deformation mechanisms in hydrogels

Daniel G. T. Strange,¹ Timothy L. Fletcher,¹ Khaow Tonsomboon,¹ Helen Brawn,¹ Xuanhe Zhao,² and Michelle L. Oyen¹

¹Engineering Department, Cambridge University, Trumpington St., Cambridge CB2 1PZ, United Kingdom

²Soft Active Materials Laboratory, Department of Mechanical Engineering and Materials Science, Duke University, Durham, North Carolina 27708, USA

(Received 9 November 2012; accepted 8 January 2013; published online 24 January 2013)

Hydrogels have applications in drug delivery, mechanical actuation, and regenerative medicine. When hydrogels are deformed, load-relaxation arising from fluid flow—poroelasticity—and from rearrangement of the polymer network—viscoelasticity—is observed. The physical mechanisms are different in that poroelastic relaxation varies with experimental length-scale while viscoelastic does not. Here, we show that poroviscoelastic load-relaxation is the product of the two individual responses. The difference in length-scale dependence of the two mechanisms can be exploited to uniquely determine poroviscoelastic properties from simultaneous analysis of multi-scale indentation experiments, providing insight into hydrogel physical behavior. © 2013 American Institute of Physics. [<http://dx.doi.org/10.1063/1.4789368>]

Hydrogels are increasingly being used as biomaterials and scaffolds,¹ substrates for cell culture,² and soft flexible actuators.³ Hydrogels are polymer networks swollen with water and they can exhibit substantial time-dependent relaxation. The relaxation results from the frictional drag of interstitial fluid through the polymer network—poroelasticity—and the intrinsic viscoelasticity of that polymer network. These effects can be understood using poroviscoelastic (PVE) theory.^{4,5}

Mechanical characterization of PVE materials is challenging for a number of reasons. Indentation is an advantageous method of testing hydrogel materials, as it avoids the need to grip and carefully manufacture experimental samples, although it can be difficult to analyze the resulting data to obtain material properties. Other common techniques include confined and unconfined compression. At a minimum, characterization requires describing the elastic (shear modulus G_∞ and drained Poisson's ratio ν), poroelastic (hydraulic permeability κ), and viscoelastic material parameters (normalized shear and bulk relaxation functions, $G(t)/G_\infty$ and $K(t)/K_\infty$). Solutions for creep and relaxation in Laplace space can be derived using the correspondence principle for problems where analytical poroelastic solutions already exist and fit to experimental data using numerical methods.^{5,6} Inverse finite-element (FE) methods can also be used to identify PVE parameters although these methods are time-consuming.^{7–10} In both cases, it is difficult to intuitively understand the effects of added viscoelastic behavior to a poroelastic problem. Furthermore, there is no guarantee that unique PVE parameters can be identified from a single test, without *a priori* assuming parameter values.¹¹

Scaling arguments can be used to differentiate between poroelastic and viscoelastic relaxation.¹² Viscoelastic relaxation results from rearrangements of the polymer network; if the experimental length-scale is much larger than the polymer mesh size, the time-constant of viscoelastic relaxation will be independent of the geometry of the test.¹³ The load-relaxation of a viscoelastic material, $P_{VE}(t)$, indented with

different sized indenters will be a function of time t and $R^{1/2}h^{3/2}$, where R is indenter radius and h is depth (Fig. 1),

$$\frac{P_{VE}(t)}{R^{1/2}h^{3/2}} = f(t). \quad (1)$$

In contrast, length-scale effects are inherent in the response of a poroelastic material.¹³ The rate of fluid flow through the network is related to the size of applied pressure gradient.¹⁴ The load-response of a poroelastic material, $P_{PE}(t)$, indented with different-sized indenters will vary quadratically in time with contact radius, $a = \sqrt{Rh}$, such that

$$\frac{P_{PE}(t)}{R^{1/2}h^{3/2}} = f\left(\frac{t}{a^2}\right). \quad (2)$$

In this paper, an agar hydrogel was characterized using multi-scale indentation, demonstrating scale-dependent relaxation. Indentation load-relaxation testing was carried out on 3% agar as follows: 3.1 mm, 7.95 mm, and 12.65 mm radius spheres were displaced into the gels to an indentation strain, $\varepsilon = \sqrt{0.2h/R}$, of 0.05 (see supplementary information for full methods).¹⁵ The experiments indicate that agar gels exhibit substantial scale-dependent relaxation: when the

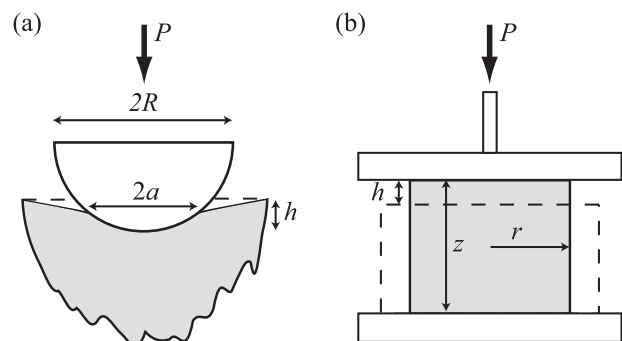


FIG. 1. Diagram showing displacement h , and load P , applied during (a) spherical indentation with tip radius R , and contact radius a , and (b) unconfined compression with cylinder radius r , and height z .

mean load-relaxation curves for three indenter sizes are normalized by the indenter geometry and plotted against time (Eq. (1); Fig. 2(a)) the trends of each curve are offset in time. When the normalized load-relaxation curves are plotted against t/a^2 (Eq. (2); Fig. 2(b)), the curves collapse onto a single curve, indicating substantial poroelastic behavior. At short times, the results do not normalize ideally, either due to differing degrees of poroelastic relaxation occurring during ramp loading or from the effects of viscoelastic behavior.¹⁶ Without further analysis, it is not possible to differentiate between poroelastic and viscoelastic contributions to the relaxation responses.

It was postulated that these viscoelastic and poroelastic contributions could be separated. Poroelastic relaxation results in a change in compressibility of the material, which can be represented by a change in Poisson's ratio from the undrained ν_u to the drained Poisson's ratio, ν .¹⁴ It does not affect the shear modulus of a fully hydrated material.⁵ It was assumed that viscoelastic relaxation does not affect Poisson's ratio, which is equivalent to assuming that the normalized shear ($G(t)/G_\infty$) and bulk ($K(t)/K_\infty$) relaxation functions are equal.¹⁷ Furthermore, it was assumed that the viscoelastic relaxation functions took the form $G(t) = G_\infty + \sum G_i \exp(-t/\tau_i)$ where G_i and τ_i are constants.

Using these assumptions, a relationship for PVE relaxation in terms of separate poroelastic and viscoelastic relaxation mechanisms was developed with analogy to an unconfined compression experiment. At any instant, the response of a material undergoing unconfined compression can be represented in terms of the elastic stiffness: $E_{\text{eff}}(t) = P(t)z/hA$, where $P(t)$ is the current load, h is the compression depth, A is the area, and z is the height of the cylinder. Invoking isotropic elasticity, $E_{\text{eff}}(t) = 2G_{\text{eff}}(t)[1 + \nu_{\text{eff}}(t)]$, where $G_{\text{eff}}(t)$ is the effective shear stiffness and $\nu_{\text{eff}}(t)$ is the effective Poisson's ratio, i.e., the radial strain divided by the applied axial strain. For a purely viscoelastic material with constant Poisson's ratio, it can be shown that $P_{\text{VE}}(t)/P_\infty = G_{\text{eff}}(t)/G_\infty$, where $P_{\text{VE}}(t)$ and P_∞ are the viscoelastic and elastic load-responses. Similarly for a purely poroelastic material, it can be shown that $P_{\text{PE}}(t)/P_\infty = (1 + \nu_{\text{eff}}(t))/(1 + \nu)$, where $P_{\text{PE}}(t)$ is the poroelastic load-response. By analogy, a PVE material will behave according to $P(t)/P_\infty = G_{\text{eff}}(t)(1 + \nu_{\text{eff}}(t))/(G(1 + \nu))$. Therefore,

$$P(t) = \frac{P_{\text{VE}}(t)P_{\text{PE}}(t)}{P_\infty}, \quad (3)$$

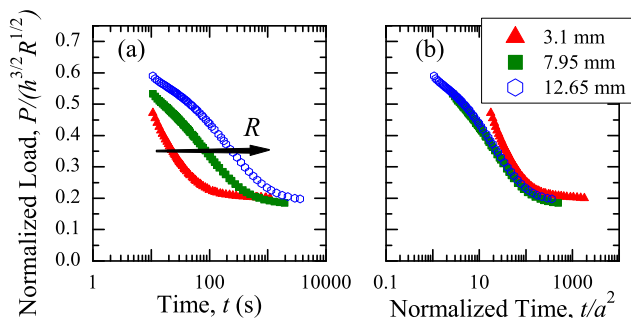


FIG. 2. Mean load-relaxation curves obtained from spherical indentation of agar (3%) with three different indenter radii. Normalized load is plotted against (a) time and (b) time normalized by contact radius.

where $P_{\text{VE}}(t)$, $P_{\text{PE}}(t)$, and P_∞ are the viscoelastic, poroelastic, and elastic load-responses calculated from equilibrium material properties. A similar argument using the reduced modulus $E_R = 2G/(1 - \nu)$ and aggregate modulus $H_A = 2G(1 - \nu)/(1 - 2\nu)$ can be used to show that Eq. (3) holds for indentation and confined compression.

Thus, PVE relaxation is the product of poroelastic relaxation and viscoelastic relaxation. This was validated by comparing its results with load-relaxation curves simulated using ABAQUS FE software (Dassault Systmes, Vlizy-Villacoublay Cedex, France) for unconfined compression and spherical indentation experiments (comparisons were also made for confined compression, see supplementary info for results as well as full details of FE models).¹⁵ Responses were computed via Eq. (3) for the unconfined compression case using analytical solutions for $P_{\text{VE}}(t)$, $P_{\text{PE}}(t)$ and P_∞ .^{1,18} There are no analytical solutions for $P_{\text{VE}}(t)$ and $P_{\text{PE}}(t)$ ramp-hold displacement controlled indentation. Instead semi-analytical and master-curve solutions were used to calculate $P_{\text{VE}}(t)$, $P_{\text{PE}}(t)$, and P_∞ (see supplementary information).^{15,16,19,20}

Load-relaxation predicted by Eq. (3) and FE was compared for a range of viscoelastic time constants, permeabilities and Poisson's ratios, for both unconfined compression and indentation. Calculating $P(t)$ using Eq. (3) was orders of magnitude faster than calculating it using FE methods, while achieving comparable accuracy (Fig. 3). It also allows for simple visualization of when poroelastic and viscoelastic mechanisms are dominant. In cases where poroelastic relaxation completed well before viscoelastic relaxation and cases where the degree of viscoelastic relaxation was very large, PVE relaxation initially proceeded too slowly, leading to a small but observable error between the calculated and FE responses. This error arises from the assumption that poroelastic relaxation can be calculated solely from equilibrium material properties. The rate of relaxation of a purely poroelastic material depends on the consolidation coefficient, c , which is a function of κ , ν , and G_∞ . When $P_{\text{PE}}(t)$ was calculated with a consolidation coefficient that depends on the effective shear modulus (determined from viscoelastic relaxation) instead of the elastic shear modulus G_∞ (i.e., allow $c = 2\kappa G_{\text{eff}}(t)(1 - \nu)/(1 - 2\nu)$), the agreement between Eq. (3) and the PVE FE simulations was near perfect. $P_{\text{PE}}(t)$ is

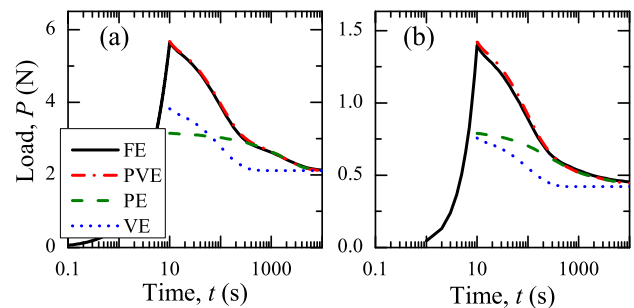


FIG. 3. PVE, poroelastic (PE), and viscoelastic (VE) relaxation with $G_\infty = 60$ kPa, $\nu = 0$, $\kappa = 7.5 \times 10^{-14}$ $\text{m}^4(\text{Ns})^{-1}$, $G_1/G_\infty = 0.2$, $G_2/G_\infty = 0.8$, $\tau_1 = 2$ s, $\tau_2 = 100$ s generated from Eq. (3) for (a) unconfined compression and (b) indentation, assuming constant consolidation coefficient $2\kappa G_\infty(1 - \nu)/(1 - 2\nu)$. The responses are compared with FE simulations.

calculated with a consolidation coefficient that depends on $G_{\text{eff}}(t)$ from here on in.

As well as providing a rapid alternative to FE methods, Eq. (3) indicates that material parameters of PVE materials can be uniquely determined using multi-scale indentation as the poroelastic component of the response is solely responsible for the scaling behavior (Eq. (2)). Load-relaxation curves obtained using multiple indenter sizes on the same material can be simultaneously fit to robustly determine the full PVE response.

This was verified by simultaneously fitting load-relaxation curves generated with forward FE models for three different indenter radii (3.1 mm, 7.95 mm, and 15.9 mm). Ramp-hold indentation experiments were simulated with a ramp time of 10 s to an indentation strain of 0.05 with a hold time of 3600 s. Gaussian noise (5% of the current load) was added to the generated load-relaxation curves in order to simulate adverse experimental conditions.²¹ The material parameters of the base model were chosen to be representative of a hydrogel such as agar ($G_{\infty} = 60$ kPa, $\nu = 0.0$, $\kappa = 7.5 \times 10^{-14}$ m⁴(Ns)⁻¹, $G_1/G_{\infty} = 1$, $\tau_1 = 100$ s). The permeability, κ was also varied from 1×10^{-15} to 1×10^{-12} , ν from 0.00 to 0.40, and τ_1 varied from 10 to 1000 ensuring that poroelastic and viscoelastic relaxations occurred concurrently, in order to test the robustness of the method. Simulations of materials with multiple viscoelastic Prony series terms were also examined.

PVE parameter identification of multi-scale forward FE models was excellent. Shear moduli were identified to be within 6%, Poisson's ratios to be within 0.08, permeabilities to be within 28%, and viscoelastic parameters (G_1 , τ_1) to be within 14%. The multi-scale approach was particularly effective, compared with fitting a single indent, when the equation was fit to a forward FE model with fewer or more Prony series terms. Poroelastic material properties were reliably identified, and the viscoelastic response was determined using the available viscoelastic parameters.

This approach was used to uniquely determine PVE material parameters from multi-scale indentation of agar. A PVE model with one viscoelastic Prony series term was simultaneously fit to the average load-relaxation curves shown in Fig. 2, using Eq. (3). A fit to the experimental data could only be obtained if Poisson's ratio was allowed to tend towards -1 . The identified parameters were $G_{\infty} = 98$ kPa, $\nu = -0.70$, $\kappa = 1.1 \times 10^{-13}$ m⁴(Ns)⁻¹, $G_1/G_{\infty} = 0.12$, $\tau = 309$ s. Increasing the number of Prony series parameters from one to three provided a negligible improvement in the accuracy of the fit (the smallest R^2 value increased from 0.976 to 0.983) and the values of G_{∞} , ν , and κ changed by 5% or less. Regardless of the number of Prony series parameters, the identification was insensitive to the initial guesses of parameters.

The identified PVE parameters were compared with direct measurements of equilibrium elastic modulus E_{∞} , drained Poisson's ratio ν , and permeability κ measured with unconfined compression testing and direct permeability measurements. The permeability of the gels directly measured using a permeometer, $\kappa = 5.1 \pm 0.9 \times 10^{-14}$ m⁴(Ns)⁻¹, compares well to the value identified from indentation tests. However, E_{∞} (unconfined compression: 82.2 ± 3.8 kPa, indentation: 58.8 kPa) and ν (0.17 ± 0.03) differed from the parameters identified from indentation measurements (Fig. 4).

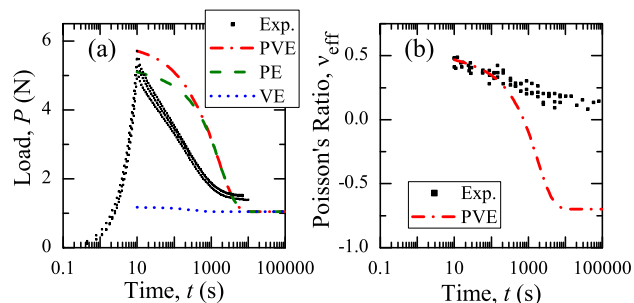


FIG. 4. Experimental unconfined compression data (Exp.) of agar (3%) showing change in load (a) and effective Poisson's ratio (b) with time. The data are compared with PVE predictions using parameters identified from multi-scale indentation which are shown as dashed and dotted lines. (Fig. 2).

The identified parameters were also used to predict the response of the material under unconfined compression and compared to experimental measurements of $P(t)$ and $\nu_{\text{eff}}(t)$ (Fig. 4). The total amount of relaxation, P_{∞}/P_0 and time to equilibrium, predicted from indentation parameters, were comparable to unconfined compression measurements, although the initial rate of relaxation differs substantially. The relaxation predicted by the PVE model is dominated by the identified poroelastic relaxation, with the large change of Poisson's ratio from the undrained Poisson's ratio of 0.5 to the drained Poisson's ratio of -0.7 . In contrast, viscoelastic relaxation contributes to a much smaller fraction of the total deformation.

Given that the approach correctly identified PVE parameters from multi-scale forward FE simulations, it is unlikely that agar demonstrates linearly isotropic PVE material behavior. Poroelastic and PVE materials with differing compressive and tensile moduli can exhibit much greater relaxation ratios than isotropic poroelastic materials, when the compressibility of the material changes from the undrained ($\nu_{\text{eff}} = 0.5$) to drained states (in this case, $\nu = 0.17$).^{18,22} Although tensile-compressive nonlinearities have not previously been reported for agar hydrogels, they are physical hydrogels and entanglements between chains could potentially stiffen in tension, and 'give' in compression. Regardless, here the identified permeability (from indentation) correlates well with direct permeability measurements.

The key finding from this work is that poroelastic and viscoelastic responses are separable for compression and indentation testing. The responses may separate for other testing modes. An analogous case is found for some nonlinearly viscoelastic materials, for which the relaxation function can be separated into a time-dependent and strain-dependent component.^{23,24} Just as is the case here, the material response is the product of the two individual responses. This finding suggests an approach to identify PVE material properties, which has been demonstrated here with forward FE simulations and experiments on an agar hydrogel, using multi-scale indentation. In retrospect, it is perhaps not surprising that the two physical mechanisms (poroelasticity and viscoelasticity) can be decoupled, since one is scale-dependent and the other is not, and one is solely a hydrostatic deformation while the other is not.

In summary, a relationship predicting PVE load-relaxation from separate poroelastic and viscoelastic

parameters has been derived, that has comparable accuracy to FE methods. The approach can be used as a rapid alternative to inverse FE methods, reducing computational time from hours to milliseconds, even for cases where no analytical solutions exist. Furthermore, the relationship provides a means for simple visualization of when poroelastic or viscoelastic mechanisms are dominant.

D.G.T.S. acknowledges funding from the Cambridge Commonwealth Trust. X.Z acknowledges support from NSF (CMMI-1253495, CMMI-1200515, and DMR-1121107).

- ¹D. G. Strange and M. L. Oyen, *J. Mech. Behav. Biomed. Mater.* **11**, 16 (2012).
- ²B. Trappmann, J. Gautrot, J. Connelly, D. Strange, Y. Li, M. Oyen, M. Stuart, H. Boehm, B. Li, V. Vogel *et al.*, *Nature Mater.* **11**, 642 (2012).
- ³X. Zhao, J. Kim, C. A. Cezar, N. Huebsch, K. Lee, K. Bouhadir, and D. J. Mooney, *Proc. Natl. Acad. Sci. U.S.A.* **108**, 67–72 (2011).
- ⁴M. A. Biot, *J. Appl. Phys.* **27**, 459 (1956).
- ⁵A. Mak, *J. Biomech. Eng.* **108**, 123 (1986).
- ⁶S. K. Hoang and Y. N. Abousleiman, *J. Appl. Phys.* **112**, 044907 (2012).
- ⁷J. E. Olberding and J.-K. Francis Suh, *J. Biomech.* **39**, 2468 (2006).
- ⁸J. Noailly, H. Van Oosterwyck, W. Wilson, T. M. Quinn, and K. Ito, *J. Biomech.* **41**, 3265 (2008).

- ⁹S. Kalyanam, R. Yapp, and M. Insana, *J. Biomech. Eng.* **131**, 081005 (2009).
- ¹⁰K. Liu and T. C. Ovaert, *J. Mech. Behav. Biomed. Mater.* **4**, 440 (2011).
- ¹¹M. Galli, E. Fornasiere, J. Cugnoli, and M. L. Oyen, *J. Mech. Behav. Biomed. Mater.* **4**, 610 (2011).
- ¹²X. Zhao, N. Huebsch, D. J. Mooney, and Z. Suo, *J. Appl. Phys.* **107**, 063509 (2010).
- ¹³Y. Hu, X. Zhao, J. Vlassak, and Z. Suo, *Appl. Phys. Lett.* **96**, 121904 (2010).
- ¹⁴H. Wang, *Theory of Linear Poroelasticity: With Applications to Geomechanics and Hydrogeology* (Princeton University Press, 2000).
- ¹⁵See supplementary material at <http://dx.doi.org/10.1063/1.4789368> for full methods.
- ¹⁶D. G. T. Strange, “Mechanics of biomimetic materials for tissue engineering of the intervertebral disc,” Ph.D. dissertation (Cambridge University, 2012).
- ¹⁷R. S. Lakes, *Viscoelastic Materials* (Cambridge University Press, 2009).
- ¹⁸B. Cohen, W. Lai, and V. Mow, *J. Biomech. Eng.* **120**, 491 (1998).
- ¹⁹J. Mattice, A. Lau, M. Oyen, and R. Kent, *J. Mater. Res.* **21**, 2003 (2006).
- ²⁰J. Hay and P. Wolff, *J. Mater. Res.* **16**, 1280 (2001).
- ²¹M. Galli and M. L. Oyen, *Comput. Model. Eng. Sci.* **48**, 241 (2009).
- ²²C. Huang, M. Soltz, M. Kopacz, V. Mow, and G. Ateshian, *J. Biomech. Eng.* **125**, 84 (2003).
- ²³W. Findley, J. Lai, and K. Onaran, *Creep and Relaxation of Nonlinear Viscoelastic Materials: With an Introduction to Linear Viscoelasticity* (Dover, New York, 1989).
- ²⁴M. Oyen, R. Cook, T. Stylianopoulos, V. Barocas, S. Calvin, and D. Landers, *J. Mater. Res.* **20**, 2902 (2005).